Time screening optimization algorithm for ROSAT PSPC/HRI observations

Bocchino F., Barbera M., and Sciortino S.
Istituto ed Osservatorio Astronomico "G.S. Vaiana", Palermo, Italy

Abstract

ROSAT PSPC/HRI observations are characterized by intervals with significant background count-rate enhancements mainly due to the particle or solar scattered radiation background components. We have developed an algorithm for time screening ROSAT PSPC/HRI observations in order to maximize the signal to noise (SNR) ratio of faint point-like sources. The algorithm has been tested on real and simulated data in order to find the parameters that optimize its functionality. In the case of a crowded PSPC field pointed to the Pleiades open cluster, a typical SNR gain of $\sim 20\%$ with respect to the unscreened case is obtained for faint sources with a cut of 6% of the total exposure time. This algorithm although presently tailored for the ROSAT PSPC/HRI observations can be easily generalized to the analysis of other X-ray detectors' data.

1 Introduction

This poster describes a procedure to screen out the high background intervals from X-ray observations done with the ROSAT PSPC or HRI. Aim of this screening procedure is to find a trade off between minimizing the excess background and maximizing the accepted time interval, in order to maximize the signal-to-noise ratio of the sources.

Two major background anomalies that may cause a decrease in signal to noise ratio of field sources can been identified in the background light curve of a ROSAT PSPC or HRI observations (see **Figure 1**), namely **high particle background** as identified by high master veto count-rate (only for PSPC observations) and **short term enhancements** (STE).

Our approach differs from previous recipes suggested from Snowden et al (1992, 1993) because it is **model independent**. We do not attempt to model the physical origin of the contributions, but we try to eliminate them on the basis of their effect on the signal-to-noise ratio (SNR) of point sources in the field of view.

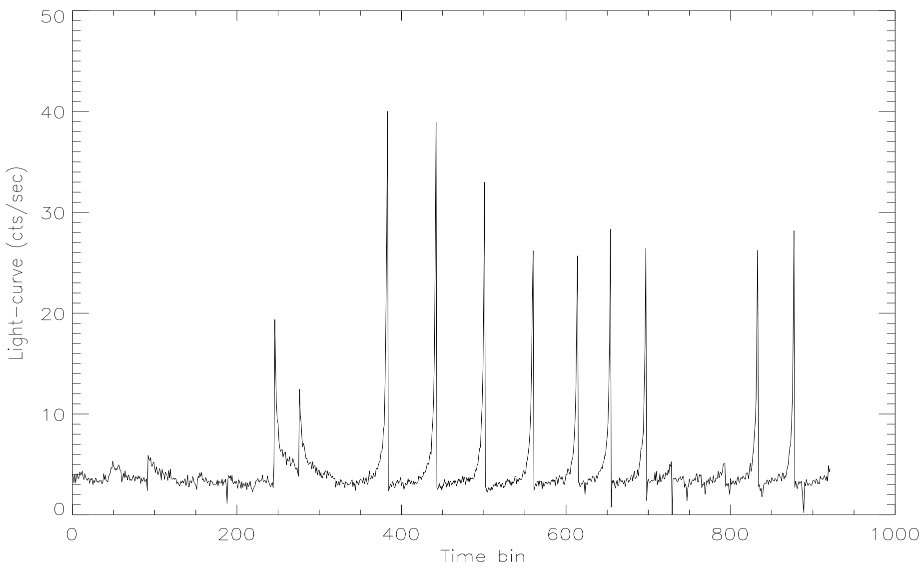

Figure 1: Background light curve of a PSPC field pointed towards the Pleiades open cluster. A large number of steep background enhancements are present along the entire $\sim$ 40.000 sec observation interval.

2 High Particle Background (PSPC only)

Snowden et al. (1992, hereafter S92) have conducted a detailed analysis on the particle component of the ROSAT PSPC background. They find a correlation between the Master Veto (MV) count-rate (count-rate detected by the anti-coincidence detector assembly), and the Particle Background (PB) of the PSPC (measured with closed entrance window).

Studying a PSPC pointed observation of the Vela supernova remnant (Bocchino, Maggio & Sciortino 1994), we have verified that the PSPC dead-time is negligible up to MV count-rate equal to 250 cts/s. Beyond that, significant dead time of the PSPC electronics may occur, resulting in a drop of the accepted X-ray events count-rate. S92 found that, if the MV rate is ≤ 250, the residual accepted PSPC particle background count-rate is below **1.3 cts/s**: this is to be compared with the **minimum** and the **typical** PSPC cosmic background rate of $\sim$ **5 cts/s** and $\sim$ **12 cts/s**, respectively.

On the basis of these considerations, **we have decided to retain all observation intervals where the MV count-rate is below 250 cts/s**. This choice is not very restrictive in terms of rejected time (less then 1% according to S92) and avoids including possible observation time intervals where the instrument is subject to high electronics dead-time that may introduce fake X-ray count-rate drops. As we have seen, setting a threshold to MV count-rate equal to 250 cts/s also sets an upper limit to the relative contribution of the PB component to the total PSPC background equal to 25%, with a more typical value of 10%.

This choice differs from the suggested threshold of 170 cts/s of S92. We have verified that adopting the Snowden's threshold results in an excessive temporal cut on the light-curve, and a sistematic decrease of point sources SNR.

3 Short term enhancements

A typical background light-curve of a ROSAT PSPC or HRI observation is characterized by occasional steep enhancements in total accepted event count-rate. In **Figure 1** for example, it is shown the light curve of a PSPC pointed observation of the Pleiades open cluster, which shows several spikes. Some of these excess background intervals are due to solar radiation (including possible flares) scattered by the Earth atmosphere, and others identify auroral X-rays (Snowden et al 1994, S94 hereafter).

The aim of the calculation described in the following is to make up a function that needs to be maximized in order to obtain the optimal screening. This function (hereafter the **efficiency function**) is defined as the ratio of a faint source signal to noise ratio (SNR) computed in a time screened observation $(SNR)_s$ and in the entire un-screened observation $(SNR)_u$, and it depends on the amount of screened out exposure time. The following formulation is very general with respect to the choice of the background cell geometry, and it does not depend on any physical models of the background contaminations. It does only depend on the assumption that the background excesses are focused and vignetted like cosmic X-rays. Since we have reduced the unvignetted PB to less than 10% (see previous section), and since the remaining contamination is made principally of solar background (Snowden et al 1993), it turns out that this is a good approximation.

The following quantities refer to the un-screened observation:

C =	total counts in the detection cell (measured quantity)
T =	total counts in the background cell (measured quantity)
S =	source counts
B =	background counts in the detection cell
α =	fraction of source counts in the detection cell
β =	fraction of source counts in the background cell
r =	ratio of the background cell area to the detection cell area

The Unscreened Signal-to-Noise Ratio. We can thus write, following the recipe of Harnden et al. (1984) and Kashyap et al. (1994):

$$C = \alpha\ S + B \tag{1}$$

$$T = \beta\ S + r\ B \tag{2}$$

With simple algebra we can obtain from equations 1 and 2 the following expression for the source counts:

$$S = \frac{r\ C - T}{\alpha\ r - \beta} \tag{3}$$

and adopting Poissonian statistics on the measured quantities C and T we can also write the standard deviation on the source counts as:

$$\sigma_s = \frac{1}{\alpha\ r - \beta}\ \sqrt{T + r^2\ C} \tag{4}$$

We can now write the signal to noise ratio of the source for the un-screened observation:

$$(SNR)_u = \frac{S}{\sigma_s} = \frac{r\ C - T}{\sqrt{T + r^2\ C}} \tag{5}$$

and using again equations 1 and 2 it becomes:

$$(SNR)_u = \frac{S\ (r\ \alpha - \beta)}{\sqrt{S\ (\beta + r^2\ \alpha) + B\ (r + r^2)}} \tag{6}$$

The screened SNR and the Efficiency Function. If a fraction x of the total observation time is screened out the expressions for C and T screened becomes:

$$C_s = (1-x)\ \alpha\ S + B_s(x) \tag{7}$$

$$T_s = (1-x)\ \beta\ S + r\ B_s(x) \tag{8}$$

where $B_s(x)$, the total background present in the screened observation, is equal to B (see equations 1 and 2) for x equal zero (un-screened observation).

Analogously to what we have done for the un-screened observation we can derive the screened SNR:

$$(SNR)_s = \frac{S\ (1-x)\ (r\ \alpha - \beta)}{\sqrt{S\ (1-x)\ (\beta + r^2\ \alpha) + B_s(x)\ (r + r^2)}} \tag{9}$$

We can now define the efficiency function $E(x, r, \alpha, \beta, S, B)$ that need to be maximized in order to obtain the optimum screening of the observation under analysis.

$$E(x, r, \alpha, \beta, S, B) = \frac{(SNR)_s}{(SNR)_u} = \frac{(1-x)\ \sqrt{(\beta + r^2\ \alpha) + B/S\ (r + r^2)}}{\sqrt{(1-x)\ (\beta + r^2\ \alpha) + B_s(x)/S\ (r + r^2)}} \tag{10}$$

The parameters r, α, and β depend on the geometry of the source and background cells and can be tabulated once the PSF of the instrument is known as a function of the off-axis at a fixed energy. In our approach, we have chosen a circular detect cell which includes 90% of the source photons ($\alpha = 0.9$) and an annular background region whose inner radius is equal to the detect cell radius and whose area is three times the detect cell area ($r = 3$). From the integration of the PSPC point spread function (PSF) at 0.3 keV given by Hasinger et al (1994), we found for β a typical value of 0.08 for offaxis angles in the range $0' - 50'$. With these choices α, β, and r are independent on off-axis position and the only relevant parameters remain S, and B.

4 Test simulations

Before we describe operatively the screening procedure, we discuss, on the basis of simulation test results, the dependence of our screening procedure on the choice of the parameters (i.e. B, which depends on the off-axis angle, and S, the counts of the point source). For these purposes we have studied a PSPC field of the Pleiades young open cluster with nearly 40000 s total exposure time (rp200068, PI Rosner) presenting many steep background enhancements (figure 1).

Choice of S. As it is expected, the faintest sources are the most affected by background enhancements, and they require an higher fraction of screened-out time (say x_{faint}) to maximize their SNR. Hence, if x_{bright} is the correspondent fraction to obtain the maximum SNR for the brightest sources, we have $x_{bright} < x_{faint}$. Therefore, when the screening procedures is tailored to obtain maximum SNR for faint sources, more time intervals are screened out than necessary for obtaining maximum SNR for brighter sources. Nevertheless, we have verified that the screening procedure, if tailored to faint sources, usually produces also an increase in SNR for bright sources. **Since we are more interested in optimal SNR gain for faint sources rather than for the bright ones, we set S equal to the minimum number of counts required to have a statistical significant detection in the field of view.**

Choice of B. As we move outside from the center of the field of view, the width of the PSF becomes larger and the detection cell is also enlarged in order to keep constant α. This implies an increase of the background counts B that scales with the detection cell area, and an increase of the minimum number of sources counts, S, required for a statistical significant detection. In order to investigate the dependence of the screening results on S/B, we have conducted some tests on the Pleiades PSPC field under study, running the screening procedure with B and S at different off-axis.

Table 1 summarizes the results of this test. and shows that the choice of tailoring the algorithm to high offaxis angles does not affect the gain in SNR of sources at lower offaxis angles. For instance, an on-axis source (first row in table 1) would have a gain of 2% in SNR with the choice of tailoring the algorithm to $30'$ offaxis angle (column 8), which is identical to the gain which would be obtained tailoring the algorithm to the on-axis source (column 5).

Furthermore, it is evident that the screening algorithm is not very sensitive to the chosen off-axis. This shows that the increase of the detection cell size, and thus B, and the increase of the detection threshold that occurs at large off-axis, in some way compensates keeping S/B nearly constant. On the basis of these results we have chosen to tailor our screening procedure for off-axis $= 30'$ where we have the highest gain in SNR still having acceptable performances of the ROSAT PSPC both in terms of sensitivity and spatial resolution.

Table 1: Analysis of the dependence of the screening procedure on the off-axis distance where S and B are calculated. Column 1 is the chosen off-axis, column 2 gives the associated detection cell radius, column 3 is the detection threshold for that off-axis derived from a standard sensitivity map of the Wavelet detection Algorithm (Damiani et al. 1995) scaled to the observed background rate and exposure time (see section 4), column 4 gives the fraction of screened time (x), column 5 gives the ratio $(SNR)_s/(SNR)_u$ i.e. the SNR gain for the source to which the screening is tailored, columns 6, 7, and 8 give the SNR gain which would be obtained if the procedure would have been tailored to $10'$, $20'$ or $30'$ offaxis angles.

Off-axis (arcmin)	Radius (arcmin)	S (cnt/s)	x (%)	$\frac{(SNR)_s}{(SNR)_u}$	$\frac{(SNR)_s}{(SNR)_u}$ at 10'	$\frac{(SNR)_s}{(SNR)_u}$ at 20'	$\frac{(SNR)_s}{(SNR)_u}$ at 30'
0	0.475	6.7×10^{-4}	3.7	1.02	1.02	1.02	1.02
2	0.492	6.8×10^{-4}	3.9	1.02	1.02	1.02	1.02
4	0.492	6.9×10^{-4}	3.7	1.02	1.02	1.02	1.02
6	0.542	7.5×10^{-4}	3.9	1.03	1.02	1.02	1.02
8	0.592	8.2×10^{-4}	4.2	1.03	1.03	1.03	1.03
10	0.692	9.3×10^{-4}	4.5	1.03	1.03	1.03	1.03
15	0.992	1.2×10^{-3}	5.4	1.04		1.04	1.04
20	1.408	2.0×10^{-3}	5.4	1.04		1.04	1.04
25	1.875	2.2×10^{-3}	5.6	1.05			1.05
30	2.391	2.9×10^{-3}	5.6	1.05			1.05

5 The operative recipe

We proceed following these steps:

1. For each image we determine the background light curve count collection region. This is accomplished computing the 20% and 80% percentiles of the count-rate image, and retaining in the collection region the pixels which fall within this range. With this choice, we discard putative sources and possible shadows (i.e. PSPC ribs);
2. We build the background light-curve of the field summing up all pixel counts in the image mask defined in step 1, and scale it to the detection cell size at $30'$ off-axis angle. We sum up the background light-curve to obtain the background counts B;
3. We scale to the actual field observation time and background count-rate a simulated sensitivity image, derived with a Wavelet detection algorithm for a 1000 s observation with 10^{-3} $ct/(s\ arcmin^2)$ average background (courtesy of F. Damiani). From this image we compute the detection threshold of our field at $30'$ off-axis angle and use it as the source count-rate in the screening procedure. We multiply this count-rate by the exposure time in order to get the source counts S.

At this stage we have all the information necessary to run the screening procedure. We define a variable that we call **background moving threshold** and set it initially to the maximum value of the background light-curve. Step by step we decrease this variable of small amounts (say 1% of the initial value). At each step we evaluate x as the fraction of exposure time where the background count-rate is in excess of the moving threshold, and also evaluate $B_s(x)$ subtracting from B the background counts in the above "excess" background intervals. Figure 2 gives a pictorial view of the quantities calculated at each step. Given x and $B_s(x)$, the efficiency function E can be calculated. When this function gets to its maximum the screening procedure is stopped and the time intervals to be screened out are identified.

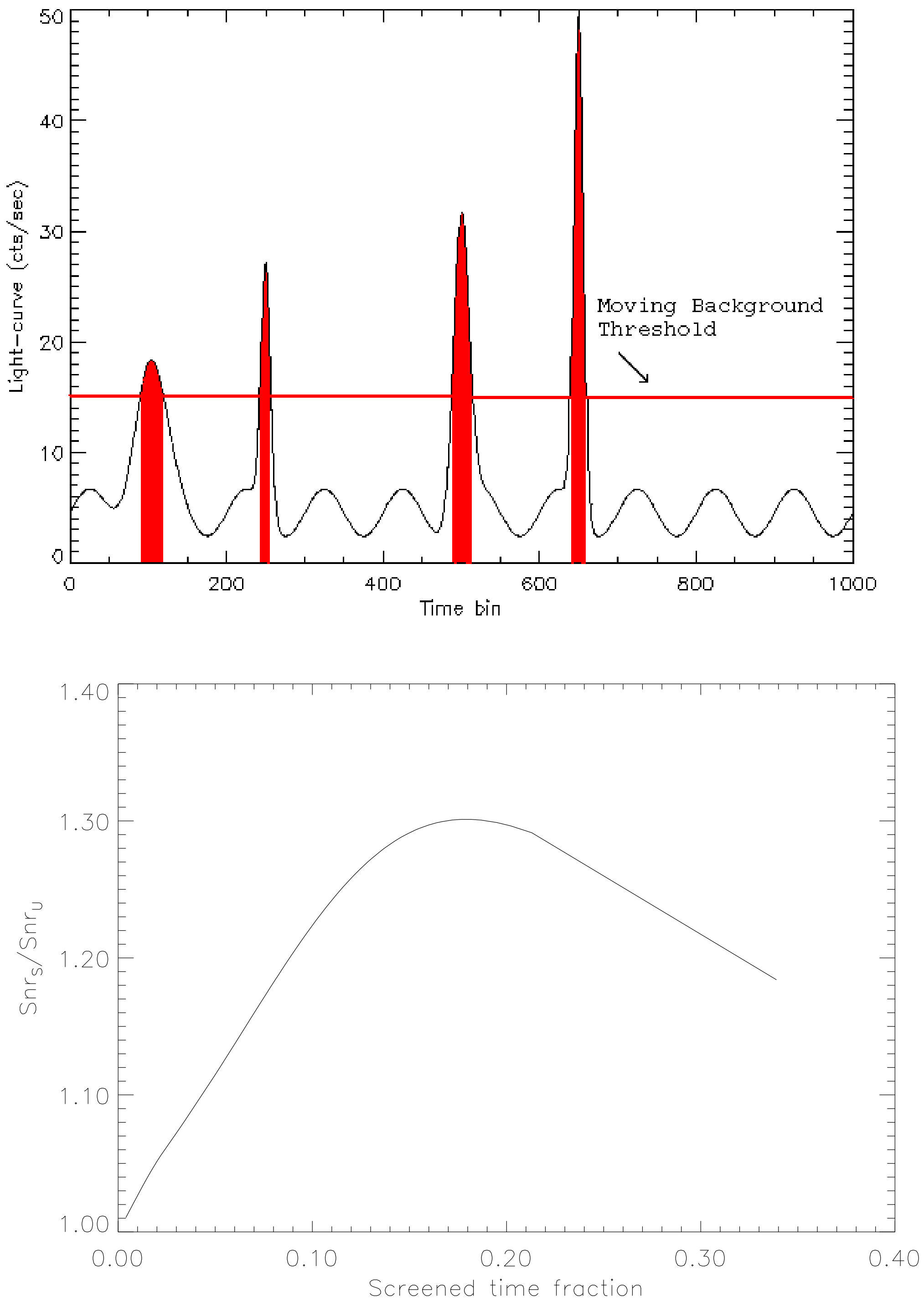

Figure 2: In this simulated background light curve **(at the top)** we put in evidence some of the relevant quantities involved in the screening procedure. The red line is the background moving threshold (BMT). The red areas represent the intervals (and thus background counts) that are screened out at this stage of the procedure. $B_s(x)$ is the integral of the light curve out of the red areas. The efficiency function is shown **at the bottom** versus the fraction of screened out time. The screening algorithm start from $x = 0$ (no screening, BMT=50 cts/s in this example) and stops at the maximum gain (here at $x = 0.18$).

6 Application to real data

To test the gain in SNR achievable with our screening code, we have used a pointed PSPC observation of the Pleiades open cluster (rp200068, PI Rosner, 43076 sec unscreened exposure). In this case, our algorithm has screened out 2828 sec (about 6% of the entire exposure time). In particular, we applied the Wavelet detection algorithm described by Damiani et al. (1995) to both the unscreened and the screened data sets, and we computed the SNR of the sources detected both in screened and unscreened observation using circular cells and r, α and β as reported in section 3.

Figure 3 shows the ratio SNR_u/SNR_s vs. SNR_u of the 93 sources having $SNR_u \geq 2.5$. Beside a statistical scattering of data points, we notice a trend for detections with low unscreened SNR to have a SNR_s/SNR_u ratio greater than one. The median of SNR_s/SNR_u for faint sources ($2.5 \leq SNR_u \leq 6$) is 1.12, whereas not much gain is obtained for brighter sources. This evidence is in good agreement with results of previous test runs (table 1) showing the advantage of tailoring the algorithm to faint sources.

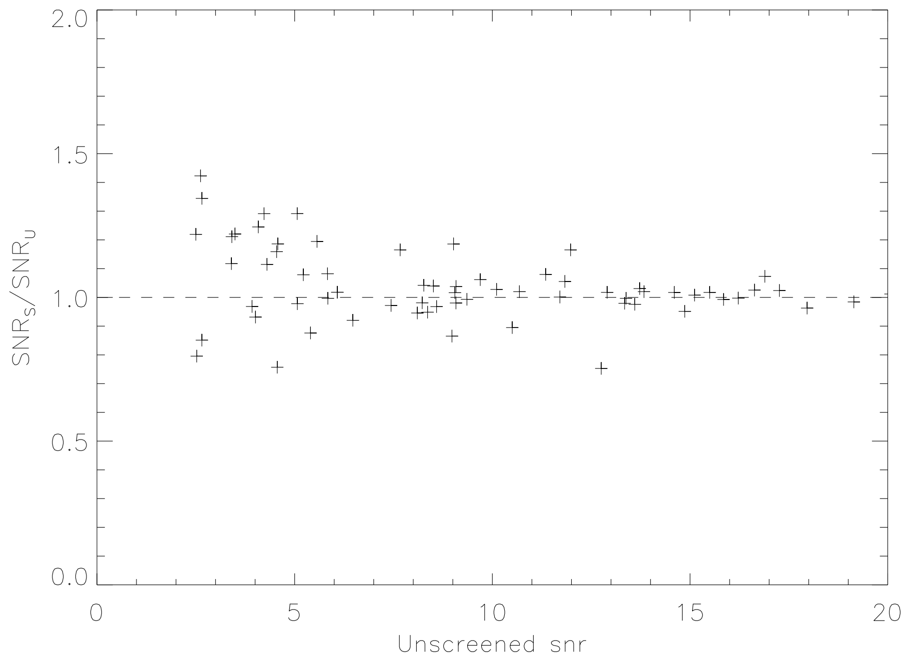

Figure 3: SNR_u/SNR_s vs. SNR_u for 93 sources detected both in screened and unscreened PSPC observation of the Pleiades open cluster.

7 The HRI case

Given its generality, the algorithm is immetiately portable to other detectors. In the case of the *ROSAT* HRI, we have used the same cell geometry, but different choise of α and β. We adopted the PSF given by David et al (1995) and we have verified that the highest value of α usable for count extraction purposes is 0.85. Beyond that value, calculation of α involves integration of the tails of the PSF, and these are poorly known, resulting in high uncertainties of the profiles.

Results of test simulations and applications to real HRI data indicate that smaller amount of screening than the PSPC case are generally required for HRI (up to 5% of the total exposure time, instead of 5-10% of the PSPC). This is due to the following fact: even though the field-of-view HRI background rate is higher that the PSPC one, the background rate **per resolution element** is smaller because the HRI has better spatial resolution, and the source detectability is less sensible to background STE's. For the same reason, the gain in SNR is also generally smaller.

References

Bocchino, F., Maggio, A., Sciortino, S., 1994, ApJ, 437, 209.
Damiani, F., Maggio, A., Micela, G. & Sciortino, S. 1995, poster at this meeting.
David, L.P., Harnden, Jr.,F.R., Kearns, K.E., & Zombeck, M.V., 1995, *"The ROSAT High Resolution Imager (HRI), US. ROSAT Science Data Center/SAO"*
Harnden, F. R. Jr., Fabricant, D. G., Harris, D. E., Schwarz, J. 1984, SAO Special Report 393
Hasinger G. Boese G., Predehl P, Turner, T.J, Yusag R, George I.M, Rohrbach G., MPE/OGIP Calibration Memo, CAL/ROS/93-015
Kashyap, V., Micela, G., Sciortino, S., Harnden, F. R. Jr., Rosner, R. 1994, in *The Soft X-ray Cosmos (AIP Conference Proceedings 313)*, Schlegel E. M. ed., p.239
Snowden, S. L., & Freiberg, M. J. 1993, ApJ, 404, 403
Snowden, S. L, McCammon, D., Burrows, D. N., & Mendenhall, J. A. 1994, ApJ, 424, 714
Snowden, S. L, Plucinsky, P. P., Briel, U., Hasinger, G. & Pfefferman, E., 1992, ApJ, 393, 819